



The HERA-B ring imaging Cherenkov system – design and performance

Jörg Pyrlík

For the HERA-B RICH Collaboration¹

University of Houston, Houston, TX 77204-5506, USA

Abstract

The Ring Imaging Cherenkov detector of the HERA-B experiment at DESY has been completed in January of 1999. Data in its final configuration were taken recently. The HERA-B RICH uses C_4F_{10} as radiator gas and a large 24 m^2 spherical mirror for imaging. The photon detector employs 2240 Hamamatsu multi-anode photomultipliers with a total of 27 000 channels. To match anode dimension (4.5 mm) and dispersion error and to solve the PMT packing problem we used a 2:1 reducing two-lens telescope in front of each PMT. The design performance of the RICH was fully reached: the average number of photons for a $\beta = 1$ particle detected in the RICH was found to be 35.4; a single-photon resolution of 0.65 mrad was reached. We used stand-alone ring finding algorithms to measure the angle and β of tracks. With the position information of the target and that of clusters in the electromagnetic calorimeter we were able to identify electrons, pions, kaons and protons. © 2000 Elsevier Science B.V. All rights reserved.

Keywords: RICH; Multi-anode PMTs; HERA-B experiment

1. Introduction

The main goal of the HERA-B experiment at DESY is to study CP violation in the B system. The B's are produced by collisions of 920 GeV halo protons with an internal multiwire target operated in parallel with the other experiments at the HERA storage ring. An average interaction rate of up to 40 MHz can be achieved [1]. The main function of the ring imaging Cherenkov counter (RICH) in HERA-B is the identification of hadrons over a large momentum range and acceptance. Identifi-

fied kaons serve as a flavor tag for the B decays in the CP-violation measurement. The overall design of the recently completed RICH and the measured performance are presented.

2. Design

2.1. Radiator

A radiator vessel made from stainless steel plates with 1 mm aluminum particle entrance and exit windows is placed about 11 m downstream of the target (see Fig. 1). Light exits the vessel through 2 mm thick UV grade Plexiglas windows. The vessel is filled with 100 m^3 of C_4F_{10} , a gas with a low dispersion of 5% in our spectral acceptance

¹ U. of Texas, Austin; U. of Barcelona, Spain; U. of Coimbra, Portugal; DESY; U. of Houston; Northwestern U.; J. Stefan Inst. and U. of Ljubljana, Slovenia.

E-mail address: pyrlík@mail.desy.de (J. Pyrlík).

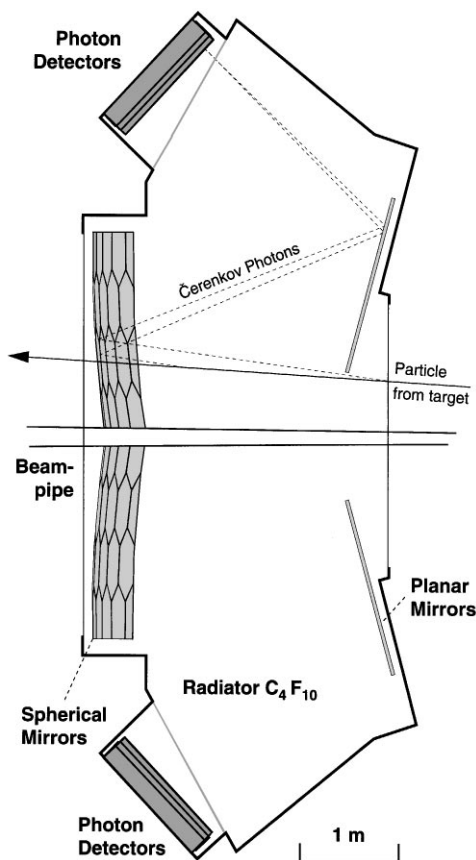


Fig. 1. Schematic of the RICH. Rays emitted by a particle and their path to the photon detector are indicated.

from 300 to 480 nm. The radiator has a refractive index of $n = 1.35 \times 10^{-3}$ and an average thickness of 2.75 m. The Cherenkov opening angle for $\beta = 1$ particles is 52 mrad. The radiator gas is being circulated in a closed system with liquification stages for cleaning and buffering. Requirements on impurities are moderate due to the operating range in the near UV and the visible part of the light spectrum.

2.2. Mirrors

The main imaging device is a spherical mirror, placed inside the radiator with the center of the sphere at the z -position the target and a radius of curvature of 11.4 m. The mirror, a 6 m by 4 m rec-

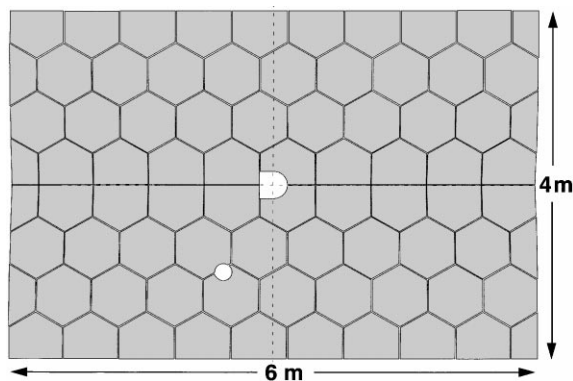


Fig. 2. Distribution of spherical mirror multigons. The holes in the center are for the proton and electron beam pipe.

tangular cutout from the sphere, is made up of 80 full or partial 7 mm thick hexagons made from Pyrex glass, coated with 200 nm aluminum and 30 nm MgF_2 (see Fig. 2). To be able to place the focal surface – a sphere with half the radius of the spherical mirror – outside of the particle flux (± 160 mrad vertically), the mirror is split horizontally and both halves are tilted by 9° away from the beam-line. A set of two planar mirrors, composed of 18 rectangular elements each, translates the focal plane conveniently to an area above and below the radiator vessel (see Fig. 1). All 80 spherical as well as the 36 planar mirrors are mounted on a rigid low mass support structure inside the radiator volume and can be individually adjusted by stepper motors from the outside. All mirrors have been aligned to better than the needed precision by surveying them inside the vessel.

2.3. Photon detector

The very high interaction rate and large multiplicity of charged tracks produces a Cherenkov light flux up to several MHz per cm^2 . We found that only photomultipliers could operate reliably for the lifetime of the experiment [2]. We therefore have abandoned all attempts to use photosensitive gas chambers as photon detector [3].

We chose Hamamatsu multi-anode PMTs with 16 anodes (R5900-00-M16) for the inner region and 4 anodes (R5900-03-M4) for the outer. A total of

1500 M16 and 750 M4 photomultipliers have been acquired. The PMTs come in a small 28 mm^2 square metal can and have a continuous $18 \times 18 \text{ mm}^2$ bi-alkali photo cathode. The anode structure is formed by metal channel dynodes (12 stages for the M16 and 10 for the M4). Both types have very low noise and allow easy single-photon detection. All PMTs were tested and an optimal high voltage has been determined for each tube.

To mount, power, and read out the photomultipliers we have developed two types of *base-boards*, one for M4 and one for M16 PMTs. Each base-board is a light tight four-layer FR4 circuit-card, $70 \times 70 \text{ mm}^2$ in size, equipped with surface mount components. The board holds four custom designed sockets and divider chains, appropriate for the type of PMT, on one side; the other side contains one (M4) or four (M16) connectors for the 16-channel readout-cards, attenuation circuitry and two daisy-chainable high-voltage connectors. The base-boards are mounted in such a way, that all PMTs are positioned on 36 mm centers (see Fig. 4).

The upper- and lower-focal surfaces have been approximated by cylinders to minimize the spherical aberrations. The cylinders are tilted by 18° to compensate for the 9° tilt of the spherical mirrors. This focal surface is approximated by seven rectangular $1.1 \times 0.4 \text{ m}^2$ super-modules following the curve of the cylinder. The supermodules are boxes containing a grid made from 1 mm thick soft iron sheet that serves as magnetic shield and mounting structure for the base-boards and the light collection system. The two types of photomultipliers have been arranged according to occupancy and

reconstruction requirements as indicated in Fig. 3. Between two and five base-boards, with their PMTs selected for similar optimal operating voltage (range 750–890 V), are powered by a single output from a 160-channel CAEN SY527 high-voltage supply.

The resolution error from dispersion in the radiator ($\sigma \approx 0.5 \text{ mrad}$) matches the error from segmentation for a 9 mm cell ($9 \text{ mm}/\sqrt{12}/f_{\text{mirror}} = 0.46 \text{ mrad}$). The dimension of a single anode of the M16 PMT is 4.5 mm. To reduce the pixel size to that of an anode and to solve the PMT packing problem, a two-lens telescope was developed consisting of a 35.3 mm^2 square plano-convex field lens ($f = 95 \text{ mm}$) and a circular 32 mm diameter bi-convex collector lens ($f = 30 \text{ mm}$) [4]. The telescope has been optimized for incidence angles of $\pm 150 \text{ mrad}$ and for an image demagnification of 2:1. Both lenses are aspherical and have been injection molded to optical quality from UV transparent acrylic. A set of 2 by 12 lens pairs is assembled in a lens module (see Fig. 4). The efficiency of the telescope has been measured to be 65%, with 15% reflection, 15% absorption and about 5% geometric loss.

The complete HERA-B RICH system contains 23808 $9 \times 9 \text{ mm}^2$ and 3008 $18 \times 18 \text{ mm}^2$ pixels, covering a total photon detection area of 2.9 m^2 .

3. Performance

3.1. Milestones

The radiator vessel was installed in the HERA-B experimental hall in early 1998. Both mirror

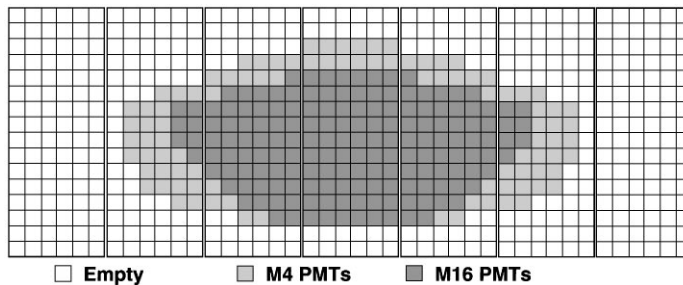


Fig. 3. Arrangement of M4 and M16 type base-boards on the 7 supermodules of the upper focal plane.

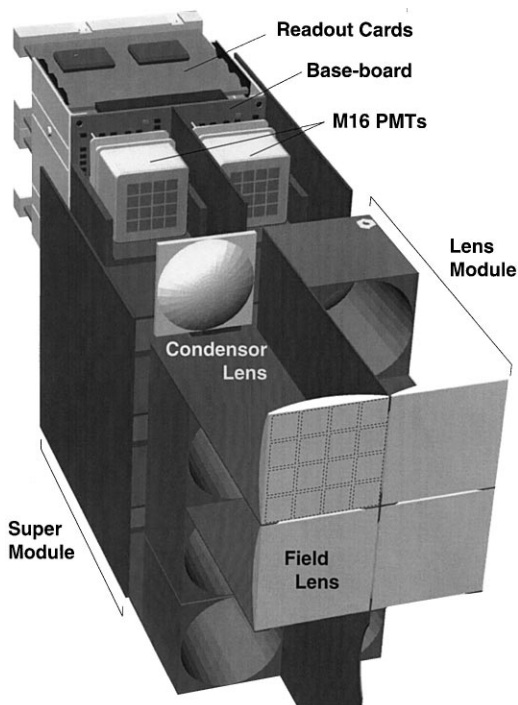


Fig. 4. Schematic of the RICH photon detector.

systems (spherical and planar) were mounted inside the vessel and aligned by surveying by April of 1998; during the same time all PMTs and the complete readout electronics was installed. The installation of the lens modules and light-tight closure of the photon detector was completed in May 1998.

The first rings with air as radiator were seen on August 19, 1998. The filling of the vessel with the final radiator gas C_4F_{10} finished in January 1999 and shortly after the first large rings were observed. The last step in running the RICH under realistic conditions was the turn-on of the solenoid magnet in May 1999.

3.2. Results

Fig. 5 shows the accumulated hits in the upper and lower RICH photon detector for a data file with approximately 3000 events, taken with the final radiator and the magnetic field on. The separation between the two types of photomultipliers

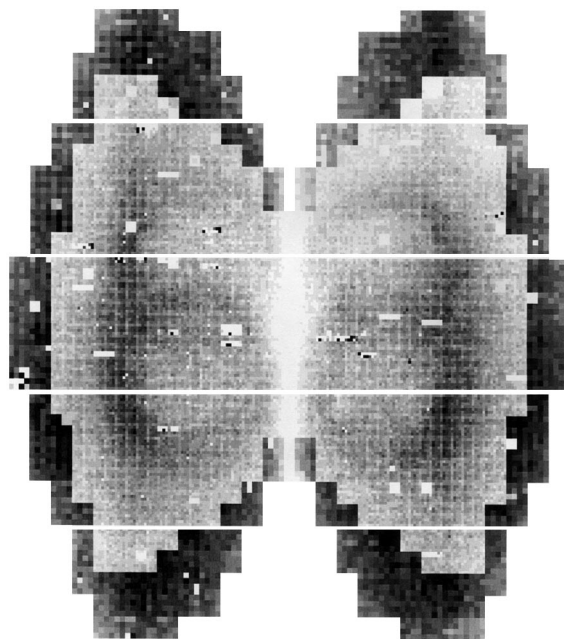


Fig. 5. Occupancy for magnet-on data. Dark areas indicate many, white areas few hits.

can be clearly seen (the M4 on the outside has a four times larger photocathode area per channel than the M16, used in the inner part). Also, apparent are the two ring patterns, caused by tracks which were produced at low angles and separated in magnetic field. The rectangular or square white areas come from non-working readout cards or PMTs. Single black pixels indicate hot channels. 90% of the bad channels have been fixed during the 1999 spring shutdown, most were caused by unplugged or wrongly connected cables.

The hit distribution in Fig. 5 agrees with MC expectations. The mean occupancy for triggered data (transverse energy in the electromagnetic calorimeter) dropped from 1155 with no magnetic field to 422 with field on. A typical event (most probable number of hits) is shown in Fig. 6, where rings can be clearly identified.

The hits in the two halves of the photon detectors can be transformed into λ , ϕ space where λ represents the declination and ϕ the azimuth of the photon directions.

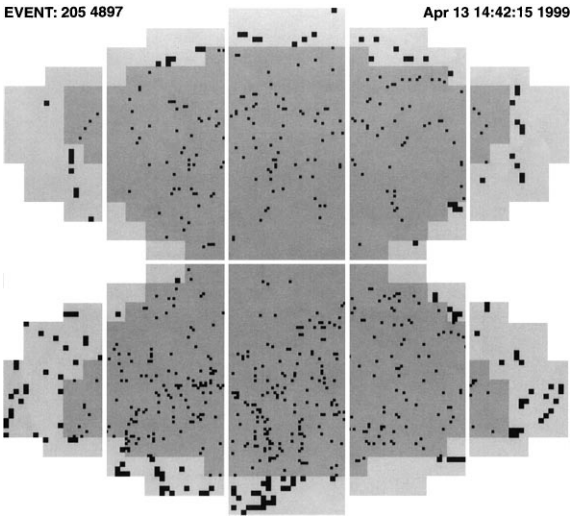


Fig. 6. Display of the raw hits of a typical event (magnet on) with 754 hits.

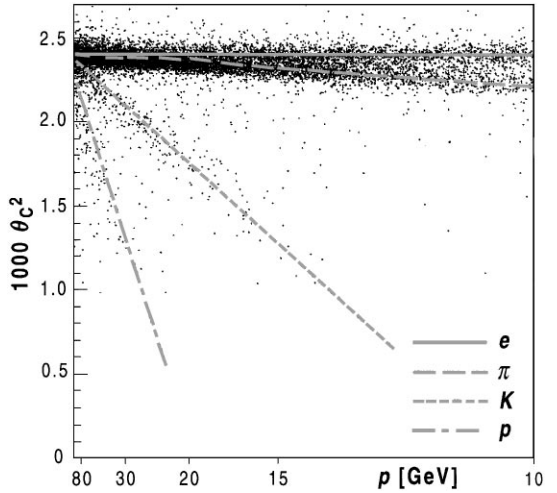


Fig. 8. Square of the ring radius versus $1/p^2$. The different particle species follow straight lines.

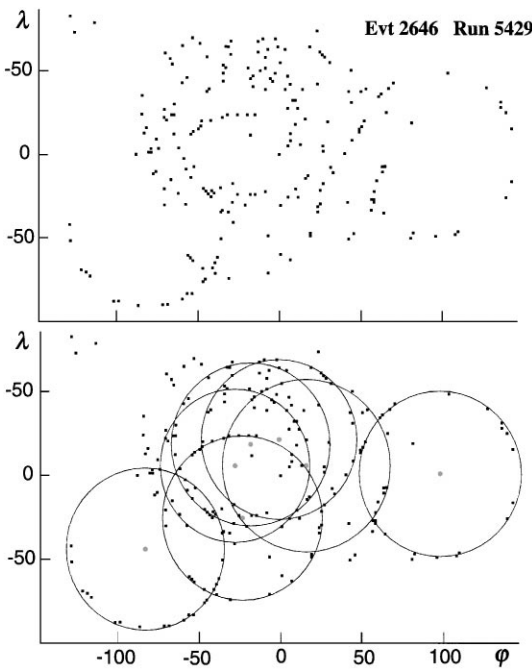


Fig. 7. Event in λ, ϕ coordinates (top), same event with reconstructed rings.

struct ring positions at reasonable CPU time requirements. An example of an event in λ, ϕ space and the corresponding found rings are shown in Fig. 7.

The main function of the RICH is hadron identification mainly for flavor tagging of B decays [5]. Due to the lack of large tracking devices in the 98/99 run, the rings in the RICH were reconstructed stand-alone. Cluster positions in the electromagnetic calorimeter were matched with track angles determined from the RICH. Assuming the target as origin, a crude momentum can be calculated. Fig. 8 shows the result of this first attempt at particle identification without tracking. Because the relation between the Cherenkov opening angle θ_c and mass and momentum of a particle is $\theta_c^2 = \theta_0^2 - m^2/p^2$, with θ_0^2 representing the $\beta = 1$ angle, particles of the same mass fall on a straight line in the representation chosen in Fig. 8.

4. Conclusion

Early data taken with the final configuration of the complete HERA-B RICH show that the system achieved the proposed performance.

Several ring finding algorithms have been developed to find rings without tracks seeds. All of them have been tested with the general HERA-B event reconstruction and are able to recon-

References

- [1] T. Lohse, Nucl. Instr. and Meth. A 408 (1998) 154.
- [2] P. Križan et al., Nucl. Instr. and Meth. A 394 (1997) 27.
- [3] J. Pyrlík et al., Nucl. Instr. and Meth. A 414 (1998) 170.
- [4] D.R. Broemmelsiek, Nucl. Instr. and Meth. A 433 (1999) 136.
- [5] P. Križan et al., Nucl. Instr. and Meth. A 433 (1999) 357.